# Deuterium Isotope Fractionation within Protonated Water Clusters in the Gas Phase

**Susan T. Graul, Mark D. Brickhouse, and Robert R. Squires***

*Contribution from the Department of Chemistry, Purdue University, West Lafayette, Indiana 47907.* *Received May 24, 1989*

**Abstract:** Ion product distributions have been analyzed for the collision-activated loss of $H_2O$, HOD, or $D_2O$ from the water clusters $(L_2O)_nL^+$ (L = H, D; $n$ = 2-4). The ionic products of collision-induced dissociation (CID) are observed to be depleted in deuterium with respect to the statistical product distributions predicted for complete randomization of H and D. The measured isotope distributions in the CID product ions are independent of collision energy within experimental error, suggesting that the observed depletion of deuterium is not the result of a kinetic effect in the unimolecular decomposition, but rather a reflection of the individual cluster structures. An equilibrium isotope effect model is proposed wherein the deuterium in the cluster preferentially migrates to the peripheral positions and localizes on the neutral water molecules in the solvent shell, rather than occupying sites in the cluster ion core, such as those on the core hydronium (lyonium) ion. Deuterium enrichment in the neutral water component of each cluster ion results in enhanced loss of deuterated neutral water upon collisional activation. The present isotope fractionation results are compared with literature data for bimolecular gas-phase H/D-exchange reactions and with condensed-phase isotope fractionation data. The observation of isotope fractionation as an equilibrium effect in stabilized gas-phase water cluster ions suggests that isotope fractionation in the bimolecular reactions between $(H_2O)_nH^+$ ions and $D_2O$ results primarily from a nonstatistical distribution of hydrogen and deuterium in the transient reaction intermediates.

Kinetic and equilibrium isotope effects are powerful tools for investigating mechanisms and energetics of reactions.[1] Isotope effects due to isotopic substitution in the solvents used for homogeneous liquid-phase reactions (solvent isotope effects)[1b,2-9] can provide detailed information about the nature of solute-solvent interactions, mechanisms of solvent assistance, and dynamics of solvation.[1,5-10] An important aspect of solvent isotope effects is isotope fractionation. Deuterium isotope fractionation in aqueous solutions is commonly characterized in terms of fractionation factors, which are phenomenological descriptions of isotope-exchange equilibria between specific hydrogens in the solute and those in the bulk solvent.[11-13] For example, the fractionation factor $\phi_s$ refers to the equilibrium constant for H/D isotope exchange of solute S with the bulk solvent (eq 1) in dilute, ideal solution

$$H_{sol} + D_{bulk} = D_{sol} + H_{bulk} \quad (1)$$

$$\phi_s = \frac{[D_{sol}][H_{bulk}]}{[H_{sol}][D_{bulk}]} \quad (2)$$

and neglecting isotope effects on activity coefficients. The experimental data for isotope fractionation between a solvated proton and bulk water are in good agreement with a model that assumes exchange between the three equivalent sites of a "lyonium" ion, $L_3O^+$ (L = H, D), and neutral water (eq 3).[11-14] The commonly

$$\tfrac{1}{3}H_3O^+(l) + \tfrac{1}{2}D_2O(l) = \tfrac{1}{3}D_3O^+(l) + \tfrac{1}{2}H_2O(l) \quad (3)$$

$$K_3 = \phi(L_3O^+)$$

accepted value for the equilibrium constants for reaction 3 is 0.69 ± 0.02 at 25 °C.[15-18] The fractionation effect has been attributed to vibrational zero-point energy differences and to entropy effects of hydration of the lyonium ion and of the counterion.[19-24] Explanations of the isotope fractionation phenomenon often emphasize the role of hydrogen bonding in weakening the force field experienced by H or D on the $L_3O^+$ moiety relative to $L_2O$,[11,12] such that the lighter atom is concentrated in the $L_3O^+$ sites. However, a fractionation factor of 0.79 was measured for the *unhydrated* lyonium ion in acetonitrile[25]—a value that is higher than that for lyonium in water, but still significantly less than unity. This observation indicates either that hydration of $L_3O^+$ is not required for isotope fractionation to occur or, alternatively, that solvation of $L_3O^+$ by acetonitrile is almost as effective as solvation by water in weakening the force field at the proton bond.

Recent studies of deuterium isotope fractionation[26-30] and related H/D-exchange reactions[31-41] involving *gas-phase* ions have

(1) (a) *Isotope Effects in Chemical Reactions*; Collins, C. J., Bowman, N. S., Eds.; Van Nostrand Reinhold: New York, 1970. (b) Schowen, R. L. *Prog. Phys. Org. Chem.* **1972**, *9*, 275. (c) Bell, R. P. *The Proton in Chemistry*; Cornell University Press: New York, 1973. (d) *Isotopes in Organic Chemistry*; Buncel, E., Lee, C. C., Eds.; Elsevier: Amsterdam, 1975; Vol. 1.

(2) (a) Gross, P.; Steiner, H.; Krauss, F. *Trans. Faraday Soc.* **1936**, *877*. (b) Gross, P.; Wischen, A. *Trans. Faraday Soc.* **1936**, *32*, 879. (c) Gross, P.; Steiner, H.; Suoss, H. *Trans. Faraday Soc.* **1936**, *32*, 883.

(3) (a) Hornel, J. C.; Butler, J. A. V. *J. Chem. Soc.* **1936**, 361. (b) Orr, J. W. C.; Butler, J. A. V. *J. Chem. Soc.* **1937**, 330. (c) Nelson, W. E.; Butler, J. A. V. *J. Chem. Soc.* **1937**, 958.

(4) (a) Noonan, E.; LaMer, V. K. *J. Phys. Chem.* **1939**, *43*, 247. (b) Kingerly, R. V.; LaMer, V. K. *J. Am. Chem. Soc.* **1941**, *63*, 3256.

(5) Gold, V. *Trans. Faraday Soc.* **1960**, *56*, 255.

(6) Kresge, A. J. *Pure Appl. Chem.* **1964**, *8*, 243.

(7) Gold, V. *Adv. Phys. Org. Chem.* **1969**, *7*, 259.

(8) Laughton, P. M.; Robertson, R. E. In *Solute-Solvent Interactions*; Coetzee, J. F., Ritchie, C. D., Eds.; Dekker: New York, 1969.

(9) Albery, W. J. In *Proton-Transfer Reactions*; Caldin, E., Gold, V., Eds.; Chapman and Hall: London, 1975.

(10) Robinson, G. W.; Thistlethwaite, P. J.; Lee, J. *J. Phys. Chem.* **1986**, *90*, 4224.

(11) Melander, L.; Saunders, W. H., Jr. *Reaction Rates of Isotopic Molecules*; Wiley-Interscience: *New York*, 1980.

(12) Kreevoy, M. M. In *Isotopes in Organic Chemistry*; Buncel, E., Lee, C. C., Eds.; Elsevier: Amsterdam, 1976; Vol. 2.

(13) Kresge, A. J.; More O'Ferrall, R. A.; Powell, M. F. In *Isotopes in Organic Chemistry*; Buncel, E., Lee, C. C., Eds.; Elsevier: Amsterdam, 1987; Vol. 7.

(14) Purlee, E. L. *J. Am. Chem. Soc.* **1959**, *81*, 263.

(15) Kresge, A. J.; Allred, A. L. *J. Am. Chem. Soc.* **1963**, *85*, 1541.

(16) Gold, V. *Proc. Chem. Soc., London* **1963**, 141.

(17) Heinzinger, K.; Weston, R. E., Jr. *J. Phys. Chem.* **1964**, *68*, 744.

(18) Salomaa, P.; Aalto, V. *Acta Chem. Scand.* **1966**, *20*, 2035.

(19) Swain, C. G.; Bader, R. F. W. *Tetrahedron* **1960**, *10*, 182.

(20) Bunton, C. A.; Shiner, V. J., Jr. *J. Am. Chem. Soc.* **1961**, *83*, 42.

(21) Halevi, A. E.; Long, F. A.; Paul, M. A. *J. Am. Chem. Soc.* **1961**, *83*, 305.

(22) Gold, V.; Grist, S. *J. Chem. Soc. B* **1971**, 1665.

(23) Gold, V.; Grist, S. *J. Chem. Soc., Perkin Trans. 2* **1972**, 89.

(24) Taylor, C. E.; Tomlinson, C. *J. Chem. Soc., Faraday Trans. 2* **1974**, *70*, 1132.

(25) Kurz, J. L.; Myers, M. T.; Ratcliff, K. M. *J. Am. Chem. Soc.* **1984**, *106*, 5631.

(26) Larson, J. W.; McMahon, T. B. *J. Am. Chem. Soc.* **1986**, *108*, 1719.

(27) Larson, J. W.; McMahon, T. B. *J. Am. Chem. Soc.* **1988**, *110*, 1087.

(28) Larson, J. W.; McMahon, T. B. *J. Phys. Chem.* **1987**, *91*, 554.

(29) Weil, D. A.; Dixon, D. A. *J. Am. Chem. Soc.* **1985**, *107*, 6859.

(30) Ellenberger, M. R.; Farneth, W. E.; Dixon, D. A. *J. Phys. Chem.* **1981**, *85*, 4.

(31) Smith, D.; Adams, N. G.; Henchman, M. J. *J. Chem. Phys.* **1980**, *72*, 4951.

(32) Adams, N. G.; Smith, D.; Henchman, M. J. *Int. J. Mass Spectrom. Ion Phys.* **1982**, *42*, 11.

(33) Smith, D.; Adams, N. G.; Alge, E. *Astrophys. J.* **1982**, *263*, 123.

(34) Smith, D.; Adams, N. G.; Alge, E. *J. Chem. Phys.* **1982**, *77*, 1261.

(35) Adams, N. G.; Smith, D. *Int. J. Mass Spectrom. Ion Phys.* **1984**, *61*, 133.

0002-7863/90/1512-631$02.50/0 

permitted additional insight into the origins and magnitude of the fractionation effect. Recently, Larson and McMahon measured gas-phase equilibrium constants for exchange reaction 4 in an ion

$$H_{3-n}D_nO^+(g) + \tfrac{1}{2}D_2O(g) = H_{2-n}D_{n+1}O^+(g) + \tfrac{1}{2}H_2O(g) \quad (4)$$

cyclotron resonance (ICR) spectrometer.[26] By combining the stepwise equilibria assayed for eq 4 for $n = 0$–2 and referencing to liquid water, they derived a fractionation factor $\phi(L_3O^+)$ of 0.79 ± 0.01 for reaction 5,[27] in excellent agreement with the value

$$\tfrac{1}{3}H_3O^+(g) + \tfrac{1}{2}D_2O(l) = \tfrac{1}{3}D_3O^+(g) + \tfrac{1}{2}H_2O(l) \quad (5)$$

obtained for lyonium ions in acetonitrile.[25] They have also applied their method to the study of deuterium isotope fractionation in $(H_2O)_2H^+$, $F^-(H_2O)$, $Cl^-(H_2O)$, and $Cl^-(HCl)$ cluster ions and concluded that rotational effects can play an important role in determining the magnitude of the fractionation factors.[27] In related studies, Smith, Adams, and Henchman determined the rate coefficients and product distributions for the gas-phase bimolecular reactions of $(H_2O)_nH^+$ and $(D_2O)_nD^+$ ($n$ = 1–4) with $D_2O$ and $H_2O$.[31,32] These H/D reactions were observed to proceed with high efficiencies, and the isotope distributions in the primary reaction product ions were reported to be essentially statistical within experimental uncertainty[31] and independent of temperature in the range 295–475 K.[32] These observations suggest that H/D exchange within the intermediate collision complexes is much faster than unimolecular dissociation.

Stabilized cluster ions can serve as useful models for intermediates in gas-phase ion–molecule reactions.[42] Partially deuterated water clusters thus correspond to the intermediates in equilibrium reaction 4 and the H/D-exchange reactions described by Smith et al.[31,32] Proton-bound water clusters ("proton hydrates") have been examined computationally at high levels of theory; the calculated minimum energy structures are shown for $(H_2O)_nH^+$ ($n$ = 2–4) cluster ions (**1**–**3**).[43-45] The presence of

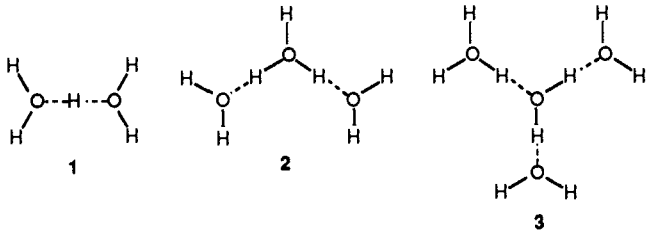

**1** **2** **3**

at least two different types of hydrogenic sites is a distinctive feature of these clusters; i.e., hydrogens can occupy either the bridging positions found in the cores of the clusters or the terminal positions in the solvent shell.[46]

In view of the reports of what appears to be a statistical product distribution for binary H/D exchange between $H_3O^+$ or $(H_2O)_nH^+$ and $D_2O$,[31,32] but measurable deuterium isotope fractionation in equilibrium reaction 4,[26,27] it is a natural question to ask whether or not hydrogen and deuterium are statistically distributed among the possible sites in partially deuterated analogues of clusters **1**–**3**. That is, can H/D isotope fractionation take place *within* the stabilized clusters, such that hydrogen or deuterium preferentially occupies either bridging or terminal positions?

In the present study, we have addressed this question by characterizing the collision-induced dissociation (CID) reactions of partially deuterated proton hydrates formed in a flowing-afterglow–triple-quadrupole instrument. In our earlier studies of methanol[47] and mixed acetonitrile–water cluster ions,[48] we showed that low-energy CID can be a useful experimental method for examining the structures of proton-bound clusters and the energy dependence of their unimolecular decompositions.[49] Herein we report accurate product distributions from CID of $d_1$–$d_4$ $(L_2O)_2L^+$, $d_1$–$d_6$ $(L_2O)_3L^+$, and $d_1$–$d_8$ $(L_2O)_4L^+$ cluster ions. The nonstatistical losses of $H_2O$, HOD, and $D_2O$ that are found from each of the clusters are interpreted in terms of an intracluster isotope fractionation process that leads to deuterium enrichment in the cluster periphery. We provide quantitative comparison of our results with the gas-phase equilibrium data for reaction 4[26,27] and with the H/D-exchange data of Smith et al.[31,32]

## Experimental Section

All experiments were carried out in a flowing-afterglow instrument equipped with an Extrel triple-quadrupole analyzer.[50] In this apparatus, ions are generated and allowed to react with neutral reagents in a 7-cm-diameter, 1-m-long, stainless steel flow tube. The ions are entrained in a constant flow of helium buffer gas (0.40 Torr, 190 STP $cm^3\ s^{-1}$) and sampled through a 1-mm-diameter orifice leading to the analyzer chamber. As the ions are borne down the flow tube, they are brought to thermal equilibrium with the buffer and reagent gases by means of thousands of nonreactive collisions and by exchange reactions. The triple quadrupole is housed in a differentially pumped analyzer chamber, which is maintained at approximately $1 \times 10^{-6}$ Torr during operation by 4- and 6-in. diffusion pumps.

Protonated water clusters $(H_2O)_nH^+$ ($n$ = 1–4) were produced by ionization of water vapor and deuterated by exchange and clustering reactions with $D_2O$ vapors added downstream in the flow tube. In order to probe the effects on isotope scrambling of the reagent mixing time (i.e., the time between addition of neutral $D_2O$ or $H_2O$ to the $(H_2O)_nH^+$ or $(D_2O)_nD^+$ clusters and sampling of the product water clusters), the $H_2O$ and $D_2O$ reagents were added at different positions along the flow tube and in reverse order.

Each of the partially deuterated water clusters in the dimer ($n$ = 2), trimer ($n$ = 3), and tetramer ($n$ = 4) series was mass-selected and subjected to collision-induced dissociation with argon target gas.[49] The relative abundances of each of the CID product ions resulting from loss of water (as $H_2O$, HOD, or $D_2O$) were carefully quantitated. Potential "spillover" of ion intensity from the $m/z \pm 1$ parent ions was prevented by maintaining the ion-selection quadrupole resolution high enough to provide base-line separation of the individual peaks. The signal intensities at 1 amu above and below the expected CID products from loss of one water molecule were monitored, and if they were not at base line, the data set was discarded. For each data set, the ion intensity recorded was the average of three or more time-averaged readings, and each data set was in turn recorded for several independent trials, on different days, by two different operators, and under somewhat varied collision conditions (collision energy 10–20 V, argon collision gas pressure $10^{-5}$–$10^{-4}$ Torr). Prior to each set of experiments, the detection system was calibrated to eliminate as much as possible any effects of mass discrimination on the fragment ion abundances (see Results for details of calibration procedure). The effects of collision energy on the fragment ion yields were monitored for several clusters by varying the laboratory collision energy and the collision gas pressure.

**Materials.** Argon gas was obtained from Air Reduction Co. at 99.995% purity, and $D_2O$ (99.8% $d$) was purchased from Aldrich Chemical Co.

## Results

Our *qualitative* observation of the product distributions from the reaction of $(H_2O)_nH^+$ ($n$ = 1–4) with $D_2O$ in the flow tube is consistent with the prediction by Smith et al.[31,32] of complete randomization of H and D within the intermediate collision complexes. We observe that at the lowest reactive conversion, when the $d_0$ cluster is still the base peak in each cluster manifold, the $d_1$ cluster is produced in greater yield than the $d_2$ cluster. This

(36) Adams, N. G.; Smith, D. *Astrophys. J.* **1985**, *294*, 165.
(37) Hunter, E. P.; Lias, S. G. *J. Phys. Chem.* **1982**, *86*, 2760.
(38) Lias, S. G. *J. Phys. Chem.* **1984**, *88*, 4401.
(39) Squires, R. R.; Bierbaum, V. M.; Grabowski, J. J.; DePuy, C. H. *J. Am. Chem. Soc.* **1983**, *105*, 5185.
(40) Grabowski, J. J.; DePuy, C. H.; Bierbaum, V. M. *J. Am. Chem. Soc.* **1985**, *107*, 7384.
(41) Grabowski, J. J.; DePuy, C. H.; Bierbaum, V. M. *J. Am. Chem. Soc.* **1988**, *105*, 2565.
(42) Castleman, A. W.; Keesee, R. G. *Chem. Rev.* **1986**, *86*, 589.
(43) Newton, M. D.; Ehrenson, S. *J. Am. Chem. Soc.* **1971**, *93*, 4971.
(44) Scheiner, S. *J. Phys. Chem.* **1982**, *86*, 376.
(45) Del Bene, J. E.; Frisch, J. J.; Pople, J. A. *J. Phys. Chem.* **1985**, *89*, 3669.
(46) Meot-Ner, M.; Speller, C. V. *J. Phys. Chem.* **1986**, *90*, 6616.
(47) Graul, S. T.; Squires, R. R. *Int. J. Mass Spectrom. Ion Proc.* **1987**, *81*, 183.
(48) Graul, S. T.; Squires, R. R. *Int. J. Mass Spectrom. Ion Proc.*, in press.
(49) For an earlier report on low-energy CID of unlabeled proton hydrates, see: Dawson, P. H. *Int. J. Mass Spectrom. Ion Phys.* **1982**, *43*, 195.
(50) (a) Graul, S. T.; Squires, R. R. *Mass Spectrom. Rev.* **1988**, *7*, 263. (b) Squires, R. R.; Lane, K. R.; Lee, R. E.; Wright, L. G.; Wood, K. V.; Cooks, R. G. *Int. J. Mass Spectrom. Ion Proc.* **1985**, *65*, 185.

indicates that the reactions cannot be described simply as a proton transfer (eq 6) nor as solvent switching (eq 7), both of which would

$$H_3O^+ + D_2O \rightarrow [H_2O\cdots H\cdots OD_2]^+ \rightarrow H_2O + HD_2O^+ \quad (6)$$

$$(H_2O)_nH^+ + D_2O \rightarrow [(H_2O)_n(D_2O)H^+] \rightarrow (H_2O)_{n-1}(D_2O)H^+ + H_2O \quad (7)$$

give the $d_2$ species as the primary product and the $d_1$ species only as a secondary product. Instead, the reaction is better described as proceeding through a relatively long-lived intermediate, in which H and D rapidly become scrambled by multiple proton (deuteron) transfer (eq 8). This can be constrasted with the related reaction

$$(H_2O)_nH^+ + D_2O \rightarrow [H_{2n}D_2O_{n+1}]^+ \rightarrow \begin{cases} H_{2n-1}D_2O_n^+ + H_2O \\ H_{2n}DO_n^+ + HOD \\ H_{2n+1}O_n^+ + D_2O \end{cases} \quad (8)$$

of the ammonia clusters $(NH_3)_nH^+$ ($n$ = 1–4) with $ND_3$ under flowing-afterglow conditions. In these reactions, we observe at low conversion that the $d_3$ cluster grows in at a comparable rate to the $d_1$ and $d_2$ clusters, suggesting that ammonia exchange (eq 10) competes with proton exchange (eq 9) and that the deuterium

$$NH_4^+ + ND_3 \rightarrow [H_3N\cdots H^+\cdots ND_3] \rightarrow NH_3 + ND_3H^+ \quad (9)$$

$$(NH_3)_nH^+ + ND_3 \rightarrow [(NH_3)_n(ND_3)H^+] \rightarrow (NH_3)_{n-1}(ND_3)H^+ + NH_3 \quad (10)$$

label is *not* completely scrambled within the intermediates.[51] The extensive H/D scrambling that occurs in reaction 8 is not a typical feature of gas-phase H/D-exchange reactions.[39-41]

To examine more carefully whether the product distributions arising from unimolecular decomposition of the intermediate collision complexes in the water system are statistical, we investigated the CID reactions of the partially deuterated proton hydrates, which were formed and collisionally stabilized in the flow tube. The partially deuterated cluster ions in the three series $d_1$–$d_4$ $(L_2O)_2L^+$, $d_1$–$d_6$ $(L_2O)_3L^+$, and $d_1$–$d_8$ $(L_2O)_4L^+$ were each in turn mass-selected at the first quadrupole of the triple-quadrupole analyzer and subjected to collisional activation with argon target gas under a range of conditions of collision energy and target gas pressure. Product ions resulting from loss of a water molecule as $H_2O$, HOD, or $D_2O$ (eq 11) were quantitated and compared

$$H_aD_bO_c^+ \xrightarrow{CID} \begin{cases} H_{a-2}D_bO_{c-1}^+ + H_2O \\ H_{a-1}D_{b-1}O_{c-1}^+ + HOD \\ H_aD_{b-2}O_{c-1}^+ + D_2O \end{cases} \quad (11)$$

to the relative abundances expected for a statistical label distribution within the reactant cluster. Our preliminary results revealed a small but reproducible deviation reflecting preferential fractionation of the deuterium to the neutral CID product. The measured product distributions were found to be the same regardless of the $D_2O$ concentration used in the flow reactor to effect H/D exchange, or of whether the labeled cluster ions were formed in the reverse order, i.e., by exchanging preformed $(D_2O)_nD^+$ clusters with added $H_2O$.

In order to rule out mass discrimination as a significant source of the observed deviations from the statistical fragment ion yields, we developed a "calibration" method that allowed us to verify that instrumental tuning was not skewing the CID product ion intensities.[52] For this calibration method, we sought a reference ion that would decompose upon collisional activation to two or more products in an accurately predictable ratio. It was also desirable to identify a reference ion that would undergo fragmentation at the laboratory collision energies used for the water system and that would produce fragment ions of masses comparable to the CID products of the water system. The most obvious choice for a calibration system seemed to be a weakly bound, isotopically labeled cluster ion for which isotope effects on cluster ion structure and dissociation are negligible under the present activation conditions. Equilibrium isotope effects arise from differences in vibrational zero-point energies and moments of inertia among the different isotopically labeled species.[19-24,27] In the water clusters, the binding sites can be occupied by hydrogen or deuterium and, because of the large relative mass differences (for D/H, a factor of 2), the vibrational frequency of a deuterium bond will differ significantly from that of a hydrogen bond. To minimize the equilibrium isotope effect, the calibrant cluster ion should be bound through an atomic species for which the relative mass difference of the isotopes is small and the vibrational frequencies are therefore similar.

The $(CH_3Cl)^+CH_2Cl$ ion proved to be a useful and easily prepared standard for this purpose.[53] Ionization of natural isotopic abundance $CH_3Cl$ in the flowing afterglow results in formation of $^+CH_2Cl$ ($m/z$ 49, 51) and the adduct ion $(CH_3Cl)^+CH_2Cl$ ($m/z$ 99, 101, 103). The latter species undergoes low-energy CID in the triple quadrupole by loss of $CH_3Cl$. Because the isotopomer of $m/z$ 101 contains exactly one $^{35}Cl$ and one $^{37}Cl$, CID of this particular ion should yield both $^+CH_2{}^{35}Cl$ and $^+CH_2{}^{37}Cl$ (eq 12).

$$\begin{bmatrix} (CH_3{}^{37}Cl)^+CH_2{}^{35}Cl \\ (CH_3{}^{35}Cl)^+CH_2{}^{37}Cl \end{bmatrix} = [^+C_2H_5{}^{35}Cl{}^{37}Cl] \xrightarrow{CID} \begin{cases} ^+CH_2{}^{35}Cl + CH_3{}^{37}Cl \\ m/z\ 49 \\ ^+CH_2{}^{37}Cl + CH_3{}^{35}Cl \\ m/z\ 51 \end{cases} \quad (12)$$

If isotope effects are important in the formation or dissociation of this cluster, the relative yield of $^+CH_2{}^{35}Cl$ and $^+CH_2{}^{37}Cl$ will deviate from the 1:1 ratio expected for a completely randomized cluster. The cluster undergoes fragmentation in the collision energy range used for the water clusters and yields CID products of masses intermediate between the masses of water dimers and trimers. The ratios measured for the product ions averaged 50.1 ± 1.0% $^+CH_2{}^{35}Cl$ and 49.9 ± 1.0% $^+CH_2{}^{37}Cl$ (the 1% uncertainty is 2 standard deviations) for a total of 30 independent experiments over a period of several months. Thus, neither equilibrium isotope effects nor kinetic isotope effects are important for this cluster under the present activation conditions.[54] The excellent reproducibility of the measurements argues against fortuitous cancellation of isotope effects and mass discrimination effects. The $(CH_3Cl)^+CH_2Cl$ calibration was, therefore, carried out prior to each set of water cluster CID experiments, and the same tuning conditions were used throughout.

With use of the $(CH_3Cl)^+CH_2Cl$ calibration method described above to set the detector tuning conditions, the relative abundances of the CID products resulting from loss of $H_2O$, HOD, and $D_2O$ from each of the partially deuterated clusters were carefully quantitated. For each cluster, multiple replicate analyses were carried out over the course of several months, involving both variations in cluster mixing time in the flowing afterglow as well as alternations in the type of exchange used to synthesize the clusters (i.e., H/D exchange for $(H_2O)_nH^+$ and D/H exchange for $(D_2O)_nD^+$). The experimental results proved to be quite

(51) Graul, S. T.; Squires, R. R. Unpublished results. See also ref 32.

(52) Although the fragment ions resulting from the loss of $H_2O$, HOD, or $D_2O$ differ by only 1 or 2 amu, the presence of a broad range of fragment ion kinetic energies and spatial distributions within the collision quadrupole (Q2), mass-dependent ion transmission between Q2 and Q3, and the need for relatively high resolution operation of Q3 all contribute to a nonneglibile potential for mass discrimination. See: (a) Dawson, P. H.; French, J. B.; Buckley, J. A.; Douglas, D. J.; Simmons, D. *Org. Mass Spectrom.* **1982**, *17*, 205. (b) Dawson, P. H.; Fulford, J. E. *Int. J. Mass Spectrom. Ion Phys.* **1982**, *42*, 195. (c) Dawson, P. H. *Int. J. Mass Spectrom. Ion Phys.* **1983**, *50*, 287.

(53) SenSharma, D. K.; deHojer, S. M.; Kebarle, P. *J. Am. Chem. Soc.* **1985**, *107*, 3757, and references therein.

(54) Primary $^{35}Cl/^{37}Cl$ isotope effects have been reported for positive and negative ions undergoing metastable and collision-activated decomposition by Cl and HCl elimination in reverse-geometry (MIKE) spectrometers: (a) Zakett, D.; Flynn, R. G. A.; Cooks, R. G. *J. Phys. Chem.* **1978**, *82*, 2359. (b) Lehman, T. A.; Crow, F. W.; Tomer, K. B.; Pedersen, L. G. *Int. J. Mass Spectrom. Ion Proc.* **1986**, *69*, 8552.

**Table I.** Product Distributions from CID of $d_1$–$d_4$ $(L_2O)_2L^+$

| parent cluster | CID product neutral | CID product ionic | stat (%)[a] | exptl (%)[b] |
|---|---|---|---|---|
| $H_4DO_2^+$ | $H_2O$ | $H_2DO^+$ | 60.0 | 57.7 ± 1.8 |
| | HOD | $H_3O^+$ | 40.0 | 42.2 ± 1.8 |
| $H_3D_2O_2^+$ | $H_2O$ | $HD_2O^+$ | 30.0 | 28.6 ± 1.5 |
| | HOD | $H_2DO^+$ | 60.0 | 58.8 ± 2.0 |
| | $D_2O$ | $H_3O^+$ | 10.0 | 12.6 ± 1.0 |
| $H_2D_3O_2^+$ | $H_2O$ | $D_3O^+$ | 10.0 | 9.5 ± 0.6 |
| | HOD | $HD_2O^+$ | 60.0 | 56.1 ± 1.0 |
| | $D_2O$ | $H_2DO^+$ | 30.0 | 34.4 ± 1.2 |
| $HD_4O_2^+$ | HOD | $D_3O^+$ | 40.0 | 36.1 ± 1.2 |
| | $D_2O$ | $HD_2O^+$ | 60.0 | 63.9 ± 1.2 |

[a] Calculated from eq 13. [b] Uncertainty corresponds to 2 standard deviations. Percents may not add to 100 due to round-off error.

**Table II.** Product Distributions from CID of $d_1$–$d_6$ $(L_2O)_3L^+$

| parent cluster | CID product neutral | CID product ionic | stat (%)[a] | exptl (%)[b] |
|---|---|---|---|---|
| $H_6DO_3^+$ | $H_2O$ | $H_4DO_2^+$ | 71.4 | 66.8 ± 1.0 |
| | HOD | $H_5O_2^+$ | 28.6 | 33.2 ± 1.0 |
| $H_5D_2O_3^+$ | $H_2O$ | $H_3D_2O_2^+$ | 47.6 | 42.3 ± 2.0 |
| | HOD | $H_4DO_2^+$ | 47.6 | 49.9 ± 2.4 |
| | $D_2O$ | $H_5O_2^+$ | 4.8 | 7.8 ± 1.4 |
| $H_4D_3O_3^+$ | $H_2O$ | $H_2D_3O_2^+$ | 28.6 | 24.6 ± 0.8 |
| | HOD | $H_3D_2O_2^+$ | 57.1 | 56.4 ± 1.8 |
| | $D_2O$ | $H_4DO_2^+$ | 14.3 | 19.0 ± 1.4 |
| $H_3D_4O_3^+$ | $H_2O$ | $HD_4O_2^+$ | 14.3 | 13.1 ± 1.0 |
| | HOD | $H_2D_3O_2^+$ | 57.1 | 52.1 ± 2.2 |
| | $D_2O$ | $H_3D_2O_2^+$ | 28.6 | 34.8 ± 2.8 |
| $H_2D_5O_3^+$ | $H_2O$ | $D_5O_2^+$ | 4.8 | 4.9 ± 1.2 |
| | HOD | $HD_4O_2^+$ | 47.6 | 43.5 ± 2.2 |
| | $D_2O$ | $H_2D_3O_2^+$ | 47.6 | 51.5 ± 2.8 |
| $HD_6O_3^+$ | HOD | $D_5O_2^+$ | 28.6 | 26.7 ± 1.6 |
| | $D_2O$ | $HD_4O_2^+$ | 71.4 | 73.3 ± 1.6 |

[a] Calculated from eq 13. [b] Uncertainty shown is 2 standard deviations. Percents may not add to 100 due to round-off error.

reproducible, typically within a few percent relative abundance. Fragmentation patterns for each of the dimeric clusters and for selected clusters from the trimer and tetramer series were examined in the low collision energy regime for evidence of energy dependence: the product ion relative abundances were analyzed for laboratory collision energies ranging from 0 to 6 V in 1- or 0.5-V steps. In all cases, there was no consistent variation in the product ion yields with increasing collision energies, although the scatter became somewhat worse at the lowest energies due to low signal-to-noise ratios. In general, the observed fragmentation patterns matched those at higher collision energies (10–20-eV laboratory frame) within the experimental reproducibility of the latter measurements. The product distributions observed for each of the cluster ions were averaged over the number of replicate measurements and are given in Tables I–III. Also shown are the product distributions expected for purely statistical decompositions, calculated from eq 13 for loss of $H_xD_yO$ from $H_aD_bO_c^+$ (see eq 11).

$$\%\ H_{a-x}D_{b-y}O_{c-1}^+ = \frac{\left[\dfrac{a!b!}{(a-x)!(b-y)!x!y!}\right]}{\left[\dfrac{(a+b)!}{(a+b-x-y)!(x+y)!}\right]} \quad (13)$$

## Discussion

The isotope fractionation that we observe in the fragmentation of the activated water clusters may be ascribed to differences in the *rates* of the various dissociation channels caused by isotopic substitution (a kinetic isotope effect, KIE), or to alteration of the ground-state *structure* of the water clusters (an equilibrium isotope effect, EIE), or to some combination of the two. Kinetic isotope effects can become serious when the difference in zero-point energies between isotopically substituted species is a significant fraction of their energy content.[55,56] This is not expected to be the case for the water system at room temperature,[32,57] much less at the elevated internal energies of the dissociating water clusters. Moreover, our search for energy dependence in the fragmentation patterns turned up to evidence for KIE's, which would most likely be revealed in the lowest collision energy region examined.[47,48,58] Thus, we attribute the fractionation effect to changes in the cluster ion structures or, more precisely, to changes in the equilibrium distribution of the isotopomeric cluster structures formed in the flow tube.

**Table III.** Product Distributions from CID of $d_1$–$d_8$ $(L_2O)_4L^+$

| parent cluster | CID product neutral | CID product ionic | stat (%)[a] | exptl (%)[b] |
|---|---|---|---|---|
| $H_8DO_4^+$ | $H_2O$ | $H_6DO_3^+$ | 77.8 | 75.2 ± 1.4 |
| | HOD | $H_7O_3^+$ | 22.2 | 24.8 ± 1.4 |
| $H_7D_2O_4^+$ | $H_2O$ | $H_5D_2O_3^+$ | 58.3 | 55.6 ± 2.0 |
| | HOD | $H_6DO_3^+$ | 38.9 | 40.4 ± 1.5 |
| | $D_2O$ | $H_7O_3^+$ | 2.8 | 3.9 ± 0.7 |
| $H_6D_3O_4^+$ | $H_2O$ | $H_4D_3O_3^+$ | 41.7 | 39.3 ± 0.9 |
| | HOD | $H_5D_2O_3^+$ | 50.0 | 50.3 ± 0.6 |
| | $D_2O$ | $H_6DO_3^+$ | 8.3 | 10.4 ± 0.8 |
| $H_5D_4O_4^+$ | $H_2O$ | $H_3D_4O_3^+$ | 27.8 | 26.8 ± 1.3 |
| | HOD | $H_4D_3O_3^+$ | 55.5 | 54.2 ± 1.3 |
| | $D_2O$ | $H_5D_2O_3^+$ | 16.7 | 19.5 ± 1.3 |
| $H_4D_5O_4^+$ | $H_2O$ | $H_2D_5O_3^+$ | 16.7 | 15.8 ± 0.8 |
| | HOD | $H_3D_4O_3^+$ | 55.5 | 53.3 ± 1.1 |
| | $D_2O$ | $H_4D_3O_3^+$ | 27.8 | 30.9 ± 1.3 |
| $H_3D_6O_4^+$ | $H_2O$ | $HD_6O_3^+$ | 8.3 | 8.0 ± 0.6 |
| | HOD | $H_2D_5O_3^+$ | 50.0 | 47.4 ± 1.0 |
| | $D_2O$ | $H_3D_4O_3^+$ | 41.7 | 44.6 ± 1.0 |
| $H_2D_7O_4^+$ | $H_2O$ | $D_7O_3^+$ | 2.8 | 2.9 ± 0.4 |
| | HOD | $HD_6O_3^+$ | 38.9 | 36.6 ± 1.4 |
| | $D_2O$ | $H_2D_5O_3^+$ | 58.3 | 60.5 ± 1.4 |
| $HD_8O_4^+$ | HOD | $D_7O_3^+$ | 22.2 | 21.5 ± 0.4 |
| | $D_2O$ | $HD_6O_3^+$ | 77.8 | 78.5 ± 0.4 |

[a] Calculated from eq 13. [b] Uncertainty shown is 2 standard deviations. Percents may not add to 100 due to round-off error.

It is of interest to note that closer inspection of the data of Smith et al.[31,33] reveals a small deviation from a purely statistical distribution of H and D in the products of the bimolecular isotope-exchange reactions, and that this deviation is in the same direction as we observe for unimolecular breakdown of the water cluster ions. It is also worth noting that the aim of the studies by Smith et al. was to examine the extent of isotope exchange within the collision complex prior to its dissociation in the bimolecular reaction and thus to compare the rate of this exchange with the rate of dissociation. Ion–molecule reaction branching ratios measured in flow reactors are typically assigned error limits of ±10 to ±30% due to uncertainties imposed by differential diffusion and mass discrimination. However, in the selected-ion flow tube instrument that was used for their studies, it is possible to correct for effects of mass discrimination and diffusion and thereby to measure branching ratios quite accurately. Thus, the small deviations of the product distributions from statistical reported by Smith et al.[31,32] need not necessarily be dismissed as random experimental error. Indeed, Henchman and Paulson have examined further this and other isotope exchange reactions and discuss the deviations observed in the branching ratio in terms of an equilibrium isotope effect and the relevant reaction hypersurface for the exchange reactions.[59]

(55) Smith, D.; Adams, N. G. *Astrophys. J.* **1980**, *242*, 424.
(56) Adams, N. G.; Smith, D. *Astrophys. J.* **1981**, *248*, 373.
(57) Henchman, M. J.; Smith, D.; Adams, N. G. *Int. J. Mass Spectrom. Ion Phys.* **1982**, *42*, 25.
(58) Forst, W. *Theory of Unimolecular Reactions*; Academic Press: New York, 1973.

**Scheme I**

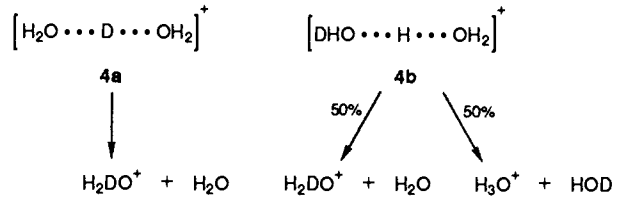


It is also important to emphasize here that the equilibrium isotope effect on the distribution of deuterium between the neutral reagent and the cluster ions in the flow tube is irrelevant in the present study. Although the cluster ions are collisionally cooled to 300 K, they are *not* at chemical equilibrium. Rather than examine the distribution of deuterium between the neutral reagent and the cluster ions, it is our goal to study the distribution of deuterium *within* each cluster and thereby to determine whether the "macroscopic" fractionation observed at chemical equilibrium is mirrored by a "microscopic" fractionation within each cluster.

If we consider the water dimer **1**, we can see that by substituting one deuterium for a hydrogen we obtain two isotopomeric structures; viz. **4a** and **4b** (see Scheme I). With four terminal positions and one bridging position, there should be 20% **4a** and 80% **4b** in a completely statistical distribution of structures. However, the condensed-phase deuterium isotope effect is such that deuterium fractionates preferentially to neutral water.[5-9] If an analogous effect is in play in the gaseous cluster ions as well, one might expect to find the terminal, "neutral water", positions enriched in deuterium and the bridging position (with its weaker force field[11,12]) enriched in hydrogen, such that the amount of **4b** in the equilibrium mixture of dimer clusters will exceed 80%.

We examine the present data in terms of two simple models: one in which the fractionation arises only from equilibrium isotope effects on the distribution of cluster ion structures and one in which the fractionation arises solely from kinetic effects on the rates of dissociation. We will show by analysis of these two models that our data are better explained in terms of an equilibrium effect. We can estimate from the experimentally observed product distributions the equilibrium distributions of cluster isotopomers for the $d_1$–$d_4$ dimer series. For these estimates, we assume that each individual isotopomer dissociates upon activation at identical rates without rearrangement and calculate the relative abundances of the isotopomers required to yield the observed product distributions. Note that although RRKM analysis of the unimolecular dissociation rates will show that this assumption is not rigorously correct, at internal energies of the cluster ions significantly above the dissociation threshold the rate differences surely will be vanishingly small. Moreover, the results of a study by Kay and Castleman of isotope fractionation in neutral water clusters formed in a supersonic free jet expansion indicate that when the isotopic constitution of the clusters is determined by the kinetics of dissociation, deuterium *enrichment* in the clusters is observed,[60] whereas our results show *depletion* of deuterium in the cluster ions. Finally, if the rates are in fact measurably different, we would expect to be able to observe systematic changes in the product ion distributions as the collision energy is varied, but the experimental distributions are reproducible for a variety of collision energies and pressures. Thus, the assumption of equal dissociation rate constants seems a valid approximation for the present study.

For the monodeuterated dimer, CID of a cluster of structure **4a** can yield only $H_2DO^+$, whereas **4b** can yield both $H_3O^+$ and $H_2DO^+$ (Scheme I). Within this model, the percent abundances of **4a** and **4b** can be derived from the experimental product distribution of $H_3O^+$ and $H_2DO^+$ by substituting into eq 14 and 15.

$$\% H_3O^+ = 0.5(\% \textbf{4b}) \quad (14)$$

$$\% H_2DO^+ = 0.5(\% \textbf{4b}) + \% \textbf{4a} \quad (15)$$

(59) Henchman, M.; Paulson, J. F. *J. Chem. Soc., Faraday Trans. 2*, **1989**, *85*, 1673.

(60) Kay, B. D.; Castleman, A. W., Jr. *J. Chem. Phys.* **1983**, *78*, 4297. We thank a reviewer for bringing this study to our attention.

**Scheme II**

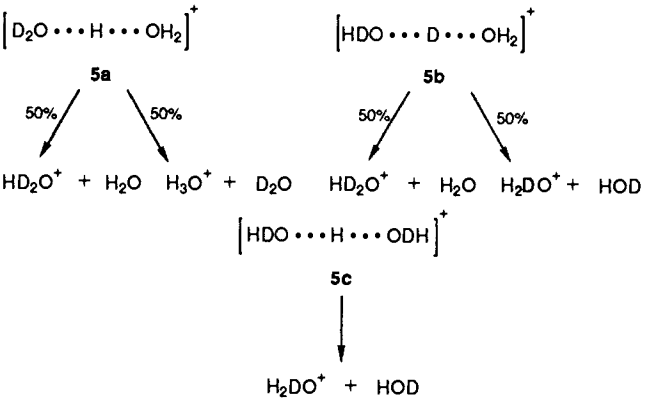


**Table IV.** Predicted Equilibrium Distribution of Isotopomeric Structures for the $d_1$–$d_4$ Water Dimers, Assuming Statistical Breakdown of the Isotopomers

| | structure | stat (%) | exptl (%) |
|---|---|---|---|
| $d_1$ | $H_2O$···D···$OH_2$ | 20.0 | 15.6 |
| | DHO···H···$OH_2$ | 80.0 | 84.4 |
| $d_2$ | $D_2O$···H···$OH_2$ | 20 0 | 25.2 |
| | DHO···D···$OH_2$ | 40.0 | 32.0 |
| | DHO···H···OHD | 40.0 | 42.8 |
| $d_3$ | $D_2O$···D···$OH_2$ | 20.0 | 19.0 |
| | $D_2O$···H···OHD | 40.0 | 49.8 |
| | DHO···D···OHD | 40.0 | 31.2 |
| $d_4$ | $D_2O$···D···OHD | 80.0 | 72.2 |
| | $D_2O$···H···$OD_2$ | 20.0 | 27.8 |

The experimentally observed yield of 42.2% $H_3O^+$ and 57.7% $H_2DO^+$ requires that the $d_1$ dimer be composed of 15.6% **4a** and 84.4% **4b**, to be compared with the 20% **4a** and 80% **4b** predicted on a purely statistical basis. Note that if the kinetic isotope effect observed by Kay and Castleman is operative for dissociation of **4b**, it should favor the channel that results in loss of $H_2O$. Under these circumstances, our estimate of the percent abundance of **4b** would actually be too low! Our values thus represent a lower limit for the deviation from a statistical distribution of the cluster isotopomers.

The three isotopomers to be considered for the $d_2$ dimer are **5a–c**. As shown in Scheme II, CID of **5a** can yield $HD_2O^+$ and $H_3O^+$, **5b** yields $HD_2O^+$ and $H_2DO^+$, and **5c** yields only $H_2DO^+$. If again we assume that isotopomers **5a–c** themselves dissociate at identical rates upon activation, then the experimental product distribution of 12.6% $H_3O^+$, 58.8% $H_2DO^+$, and 28.6% $HD_2O^+$ requires that the $d_2$ dimer be composed of 25.2% **5a**, 32.0% **5b**, and 42.8% **5c**, to be compared with 20%, 40%, and 40%, respectively, predicted on a statistical basis.

The results of these calculations for the $d_1$–$d_4$ dimer series are collected in Table IV. It is apparent from inspection of Table IV that this treatment predicts that the equilibrium distribution of structures of the clusters is depleted in the isotopomers that incorporate deuterium in bridging positions (e.g., **4a** and **5b**) and enriched in isotopomers with deuterium only in terminal positions.

To demonstrate more clearly that the fractionation observed in CID of water clusters is due to an equilibrium isotope effect, we will consider the opposite proposition: that the fractionation arises *solely* from a kinetic isotope effect operating during the CID process. This treatment assumes a purely statistical distribution of cluster isotopomers but nonstatistical breakdown patterns, i.e., differing unimolecular dissociation rates that result in enrichment of the deuterium content in the neutral CID product. The experimental product distributions (Table I) are used to calculate the required branching ratios. We assume that the *total* rate of dissociation for each isotopomer is identical (see above) but allow for breakdown of the clusters that can yield two different products to favor one product over the other. For example, for the $d_1$ dimer, we assume a statistical distribution of H and D and

**Table V.** Breakdown Ratios for the Isotopomers of the $d_1$–$d_4$ Water Dimers, Assuming a Statistical Distribution of the Isotopomers

| | dissociation reaction | | | stat (%) | exptl (%) |
|---|---|---|---|---|---|
| $d_1$ | $H_2O\cdots D\cdots OH_2$ | → | $H_2DO^+$ | 100.0 | 100.0 |
| | $DHO\cdots H\cdots OH_2$ | → | $H_3O^+$ | 50.0 | 52.8 |
| | | → | $H_2DO^+$ | 50.0 | 47.2 |
| $d_2$ | $D_2O\cdots H\cdots OH_2$ | → | $H_3O^+$ | 50.0 | 63.0 |
| | | → | $HD_2O^+$ | 50.0 | 37.0 |
| | $HDO\cdots D\cdots OH_2$ | → | $H_2DO^+$ | 50.0 | 47.0 |
| | | → | $HD_2O^+$ | 50.0 | 53.0 |
| | $HDO\cdots H\cdots ODH$ | → | $H_2DO^+$ | 100.0 | 100.0 |
| $d_3$ | $D_2O\cdots D\cdots OH_2$ | → | $D_3O^+$ | 50.0 | 47.5 |
| | | → | $H_2DO^+$ | 50.0 | 52.5 |
| | $D_2O\cdots H\cdots OHD$ | → | $H_2DO^+$ | 50.0 | 59.8 |
| | | → | $HD_2O^+$ | 50.0 | 40.2 |
| | $DHO\cdots D\cdots OHD$ | → | $HD_2O^+$ | 100.0 | 100.0 |
| $d_4$ | $D_2O\cdots D\cdots OHD$ | → | $D_3O^+$ | 50.0 | 45.1 |
| | | → | $HD_2O^+$ | 50.0 | 54.9 |
| | $D_2O\cdots H\cdots OD_2$ | → | $HD_2O^+$ | 100.0 | 100.0 |

thus that 20% of the clusters are of structure **4a** and 80% are of structure **4b**. Then we can calculate the (nonstatistical) branching ratio for breakdown of the clusters by using the experimental product distribution (42.2% $H_3O^+$ and 57.7% $H_2DO^+$) in eq 16 and 17. The 42.2% yield of $H_3O^+$ requires that $x = (42.2/80)$

$$\%\ H_3O^+ = x(\%\ \mathbf{4b}) = x(80\%) \tag{16}$$

$$\%\ H_2DO^+ = \%\ \mathbf{4a} + (1 - x)(\%\ \mathbf{4b}) = 20\% + (1 - x)(80\%) \tag{17}$$

$= 0.528$. Thus, we obtain a branching ratio for breakdown of **4b** to 52.8% $H_3O^+$ and 47.2% $H_2DO^+$. The results for each of the cluster ions are collected in Table V. There is a pronounced deviation from the statistically predicted breakdown patterns for several of the isotopomers. We note again that because this treatment is based on differing rates of unimolecular dissociation, it is to be expected that the fragmentation patterns would show energy dependence;[47,48,58] however, no such energy dependence was observed. Moreover, the trends obtained by this model are somewhat difficult to rationalize. From comparison of the $d_2$ and $d_3$ cluster data, we see the greatest deviation between statistical and experimental breakdown ratios for hydrogen-bonded isotopomers (e.g., the branching ratio of the H-bonded $d_2$ dimer deviates from statistical by 13% whereas that of the D-bonded $d_2$ dimer deviates by only 3%) and we would conclude that a bridging hydrogen is far more sensitive to its environment than a bridging deuterium. However, this is not borne out by the $d_1$ and $d_4$ cluster data, in which the deviation is slightly greater for a bridging deuterium (i.e., the branching ratio of the $d_1$ dimer deviates by only 2.8% from statistical predictions, whereas that of the D-bonded $d_4$ dimer deviates by 4.9%). Our conclusion is that a kinetic isotope effect is of less importance than the equilibrium isotope effect in determining the CID product distributions.

In view of our conclusion that the CID fractionation effect is an equilibrium isotope effect, it is of interest to see how closely our fractionation mimics that observed by Larson and McMahon in their gas-phase equilibrium study[26,27] and to compare our results with condensed-phase studies of both hydrated[14-18] and unhydrated[25] lyonium ions. This requires that we somehow express our data in a form like eq 5. The fractionation factor $\phi$ associated with the deuteration reaction 5 gives a measure of the change in the environment of the hydrogen atom relative to bulk liquid water.[12] To derive equilibrium constants from our data, we develop a model that relates the collisionally activated unimolecular decomposition of a water cluster ion to the unimolecular decomposition of a bimolecular proton-transfer reaction intermediate. Consider H/D-exchange reaction 18. When this reaction reaches

$$H_3O^+ + HOD \underset{k_2}{\rightleftharpoons} [H_4DO_2^+]^* \overset{k_1}{\rightleftharpoons} H_2DO^+ + H_2O \tag{18}$$

steady state, the equilibrium constant is given by

$$K_{18} = \frac{[H_2DO^+][H_2O]}{[H_3O^+][HOD]} \tag{19}$$

We estimate $K_{18}$ from the product distribution for CID of $[H_4DO_2^+]^*$ as shown in eq 20 and 21, recognizing that $[H_2DO^+]$

$$H_3O^+ + HOD \leftarrow [H_4DO_2^+]^* \rightarrow H_2DO^+ + H_2O \tag{20}$$

$$K'_{20} = \frac{[H_2DO^+][H_2O]}{[H_3O^+][HOD]} = \frac{(0.577)(0.577)}{(0.422)(0.422)} = 1.87 \tag{21}$$

$= [H_2O]$ and $[H_3O^+] = [HOD]$ for the CID process. The underlying assumption is that the ratio of the unimolecular dissociation rates ($k_1$ and $k_2$ in eq 18) is in fact independent of energy, as our data suggest is the case. In order to obtain the appropriate fractionation expressions, which involve only $H_2O$ and $D_2O$ (and no HOD, e.g., eq 4), we must combine results from CID of two different cluster ions that yield the same product ions upon dissociation. For the $d_0$–$d_1$ equilibrium, we have the following relationships:

$$H_3O^+ + HOD \leftarrow [H_4DO_2^+]^* \rightarrow H_2DO^+ + H_2O \tag{22}$$

$$K'_{22} = 1.87$$

$$H_3O^+ + D_2O \leftarrow [H_3D_2O_2^+]^* \rightarrow H_2DO^+ + HOD \tag{23}$$

$$K'_{23} = \left(\frac{0.588}{0.126}\right)^2 = 21.8$$

$$H_3O^+(g) + \tfrac{1}{2}D_2O(g) = H_2DO^+(g) + \tfrac{1}{2}H_2O(g) \tag{24}$$

$$K'_{24} = (K_{22}K_{23})^{1/2} = 6.38$$

We use $K'$ instead of $K$ in order to emphasize that the values of $K'$ derived with this model are *not* true equilibrium constants; for example, the value of $K'_{24}$ given above cannot be compared directly with the equilibrium constant for reaction 24 obtained by Larson and McMahon,[26,27] who derive their value directly from measurements of a true equilibrium mixture. The present value of $K'_{24}$ is simply an empirical value derived from the combination of half-reactions (cluster ion breakdown yields), and it must be corrected for the statistical factor of 9, which arises from calculation of the equilibrium constant $K'_{27}$ for purely statistical breakdown of $H_4DO_2^+$ and $H_3D_2O_2^+$:

$$H_3O^+ + HOD \leftarrow [H_4DO_2^+]^* \rightarrow H_2DO^+ + H_2O \tag{25}$$

$$K'_{25}(\text{stat}) = \left(\frac{0.60}{0.40}\right)^2 = 2.25$$

$$H_3O^+ + D_2O \leftarrow [H_3D_2O_2^+]^* \rightarrow H_2DO^+ + HOD \tag{26}$$

$$K'_{26}(\text{stat}) = \left(\frac{0.60}{0.10}\right)^2 = 36$$

$$H_3O^+(g) + \tfrac{1}{2}D_2O(g) = H_2DO^+(g) + \tfrac{1}{2}H_2O(g) \tag{27}$$

$$K'_{27} = (K_{25}K_{26})^{1/2} = 9.0$$

Because the fractionation factor is quoted with reference to liquid water, we multiply $K'_{24}$ by 0.93, the equilibrium constant for reaction 28, or equivalently the square root of the ratio of the vapor

$$\tfrac{1}{2}H_2O(g) + \tfrac{1}{2}D_2O(l) = \tfrac{1}{2}H_2O(l) + \tfrac{1}{2}D_2O(g) \tag{28}$$

$$K_{28} = 0.93$$

pressures of $D_2O$ and $H_2O$.[61-63] Thus, we have for the $d_0$–$d_1$ fractionation factor $\phi_0$

$$H_3O^+(g) + \tfrac{1}{2}D_2O(l) = H_2DO^+(g) + \tfrac{1}{2}H_2O(l) \tag{29}$$

$$\phi_0 = K_{29} = \frac{(6.38)(0.93)}{9.0} = 0.66 \tag{30}$$

The $d_0$–$d_1$, $d_1$–$d_2$, and $d_2$–$d_3$ equilibrium constants and fraction-

(61) Whalley, E. *Proc. Conf. Thermodyn. Transp. Prop. Fluids* **1975**, 15.
(62) Merliwat, L.; Botter, R.; Nief, G. *J. Chim. Phys.* **1963**, *60*, 56.
(63) Jones, W. M. *Nucl. Sci. Abstr.* **1964**, *18*, 4221.

**Table VI.** Phenomenological Equilibrium Constants and Fractionation Factors for the Stepwise Deuteration Reaction (4)

| $n$ | CID products | $K_{expt}$[a] | $K_{stat}$ | $\phi_n$[b] |
|---|---|---|---|---|
| 0 | $H_3O^+ + HOD \leftarrow [H_4DO_2^+] \rightarrow H_2DO^+ + H_2O$ | 1.87 | 2.25 | |
| | $H_3O^+ + D_2O \leftarrow [H_3D_2O_2^+] \rightarrow H_2DO^+ + HOD$ | 21.8 | 36.0 | |
| | $H_3O^+ + {}^1/_2D_2O = H_2DO^+ + {}^1/_2H_2O$ | 6.38 | 9.00 | 0.66 |
| 1 | $H_2DO^+ + HOD \leftarrow [H_3D_2O_2^+] \rightarrow HD_2O^+ + H_2O$ | 0.237 | 0.25 | |
| | $H_2DO^+ + D_2O \leftarrow [H_2D_3O_2^+] \rightarrow HD_2O^+ + HOD$ | 2.66 | 4.0 | |
| | $H_2DO^+ + {}^1/_2D_2O = HD_2O^+ + {}^1/_2H_2O$ | 0.794 | 1.0 | 0.74 |
| 2 | $HD_2O^+ + HOD \leftarrow [H_2D_3O_2^+] \rightarrow D_3O^+ + H_2O$ | 0.0287 | 0.0278 | |
| | $HD_2O^+ + D_2O \leftarrow [HD_4O_2^+] \rightarrow D_3O^+ + HOD$ | 0.319 | 0.444 | |
| | $HD_2O^+ + {}^1/_2D_2O = D_3O^+ + {}^1/_2H_2O$ | 0.0957 | 0.111 | 0.80 |

[a] Gas-phase equilibrium constants calculated from experimental product distributions (Table I). [b] Fractionation factor with respect to liquid water $(0.93)(K_{expt}/K_{stat})$.

ation factors for the water dimers determined in this way are listed in Table VI. The stepwise equilibria combine to give eq 31, with

$$H_3O^+(g) + {}^3/_2D_2O(l) = D_3O^+(g) + {}^3/_2H_2O(l) \quad (31)$$

an equilibrium constant $K_{31} = 0.39 \pm 0.04$. (The quoted uncertainty represents the change in $K_{31}$ introduced by adjusting one set of product distributions to the maximum of the error limits shown in Table I (e.g., 59.5% $H_2DO^+$ and 40.4% $H_3O^+$ from $H_4DO_2^+$) and recalculating $K_{31}$ with the resulting $K_{expt}$.) The resulting fractionation factor of $L_3O^+$ ($\phi = K_{31}^{1/3}$) is $0.73 \pm 0.02$.

We observe an overall trend of increasing fractionation factor with increasing deuterium content (see Table VI). The differences among the fractionation factors in Table VI are greater than the expected error. A similar trend is also apparent in Larson and McMahon's data, but is magnified relative to the present results; their values for $\phi_0$, $\phi_1$, and $\phi_2$ are 0.64, 0.79, and 0.97, respectively.[26,27] The present value for $\phi(L_3O^+)$ of 0.73 is lower than Larson and McMahon's value of $0.79 \pm 0.01$,[26,27] and the difference appears to be greater than the combined experimental uncertainties. Barring systematic error, a possible source of the discrepancy is the internal energies of the relevant dimer species. We expect that the thermalized (300 K) cluster ions in the flow tube have settled predominantly into the lowest energy geometry.[43-45] Upon collisional activation, the clusters are activated to relatively high internal energies (for the dimer, the center of mass collision energy is about 10 eV), and therefore they can undergo fragmentation on a faster time scale than internal rotations, in which case the product distributions reflect the "frozen" structure of the thermalized clusters. In contrast, the bimolecular reaction intermediates have excess internal energies corresponding to the solvation energy (1–1.5 eV), and at these energies the internal rotations that lead to isotope scrambling are known to be rapid compared to dissociation.[31,32] Moreover, the effective temperatures of the water cluster ions formed in the flowing afterglow and the temperature at which the ICR equilibrium reaction is carried out may differ enough to cause a measurable change in the magnitude of the fractionation effect. If this is the case, variable-temperature studies of the cluster fragmentations might reveal changes in the effective fractionation factor.

The present data suggest that the fractionation effect observed in the gas-phase equilibrium reactions of the water system arises from a nonstatistical isotope distribution within the reaction intermediates, i.e., $L_5O_2^+$. Inspection of the minimum energy structure of $L_5O_2^+$ (**1**) reveals two different types of hydrogen sites: terminal and bridging. Individual fractionation factors for these sites are defined as the equilibrium constants for eq 32 and 33, where the subscript b or t refers to bridging or terminal.[27]

$$H_b + {}^1/_2D_2O(l) = D_b + {}^1/_2H_2O(l) \qquad K_{32} = \phi_b \quad (32)$$

$$H_t + {}^1/_2D_2O(l) = D_t + {}^1/_2H_2O(l) \qquad K_{33} = \phi_t \quad (33)$$

From the experimental product distributions shown in Table I or the $L_5O_2^+$ isotopomer distributions given in Table IV, phenomenological equilibrium constants can be derived for the bridging–terminal exchange process (eq 34). For the $d_1$ dimer, after

$$H_b + D_t = D_b + H_t \qquad K_{34} = \phi_b/\phi_t \quad (34)$$

dividing by the statistical factor of 0.25, the value of $K_{34}$ is 0.76. The isotopomer distribution for the $d_2$,$d_3$, and $d_4$ dimers yields $K_{34} = 0.70$, 0.66, and 0.65. (These values differ from Larson and McMahon's estimate for $K_{34}$ of 0.44[27] primarily because of the different method used for deriving $K_{34}$; they estimate $\phi_t$ to be the geometrical mean of the $\phi$ for gaseous $L_2O$ (0.93) and $L_3O^+$ (0.79) and assign a value of 0.86.) The steadily decreasing value of the ratio $\phi_b/\phi_t$ suggests that either the value of $\phi_b$ *decreases* with increasing deuterium substitution or that the value of $\phi_t$ *increases* with deuterium content. If the former were true, the fractionation factors for the stepwise deuteration reaction 4 should decrease as deuterium content increases. However, these $\phi$ values increase (Table VI), suggesting that in fact the value of $\phi_t$ must increase. The fractionation for the terminal positions can be distinguished on the basis of whether the exchange reaction 33 involves conversion of $H_2O$ to HOD or of HOD to $D_2O$ by designating the factors as ${}^H\phi_t$ and ${}^D\phi_t$, respectively (eq 35 and 36). The $\phi_b$, ${}^H\phi_t$,

$${}^HH_t \text{ (in } H_2O) + {}^1/_2D_2O(l) = {}^HD_t \text{ (in HOD)} + {}^1/_2H_2O(l) \quad (35)$$

$$K_{35} = {}^H\phi_t$$

$${}^DH_t \text{ (in HOD)} + {}^1/_2D_2O(l) = {}^DD_t \text{ (in } D_2O) + {}^1/_2H_2O(l) \quad (36)$$

$$K_{36} = {}^D\phi_t$$

and ${}^D\phi_t$ values can be extracted by using the $L_5O_2^+$ isotopomer distributions to calculate the equilibrium constants for eq 37 and 38 and substituting into eq 39, which equates the overall fractionation factor with the individual factors for stepwise deuteration of the $L_3O^+/L_2O$ system. The values of $K_{37}$ calculated from the data for the $d_1$, $d_2$, and $d_3$ dimers are 0.76, 0.75, and 0.76. The scatter in these values is well within experimental error. Similarly, the values of $K_{38}$ from the data for the $d_2$, $d_3$, and $d_4$ dimers are 0.63, 0.63, and 0.65, respectively—again essentially identical. Upon substitution into eq 39 and with use of the present gas-phase value for $\phi(L_3O^+)$ of 0.73, we obtain $\phi_b = 0.55$, ${}^H\phi_t = 0.72$, and ${}^D\phi_t = 0.86$. The fractionation factor in the bridging position ($\phi_b$) is the lowest, indicating that this is the position with the weakest force field[11,12] and that the proton (or deuteron) at this site moves in a broad, flat potential minimum.[43-45] The excellent fit of these values to the experimental data suggests that the fractionation factor for the bridging site is less sensitive than the terminal position to deuterium substitution at the termini.

$$H_b + {}^HD_t = D_b + {}^HH_t \qquad K_{37} = \phi_b/{}^H\phi_t \quad (37)$$

$$H_b + {}^DD_t = D_b + {}^DH_t \qquad K_{38} = \phi_b/{}^D\phi_t \quad (38)$$

$$\phi(L_3O^+) = [\phi_b({}^H\phi_t)^2({}^D\phi_t)^2]^{1/5} \quad (39)$$

The product distributions for CID of $d_1$–$d_6$ $(L_2O)_3L^+$ shown in Table II again reflect fractionation of deuterium to the neutral CID product. The stepwise fractionation equilibrium constants for reaction 40 calculated from the experimental product dis-

$$H_{5-n}D_nO_2^+(g) + {}^1/_2D_2O(g) = H_{4-n}D_{n+1}O_2^+(g) + {}^1/_2H_2O(g) \quad (40)$$

**Table VII.** Phenomenological Equilibrium Constants for the Stepwise Deuteration Reaction (40)

| $n$ | CID products | $K_{expt}$[a] | $K_{stat}$ | $\phi_n$[b] |
|---|---|---|---|---|
| 0 | $H_5O_2^+ + HOD \leftarrow [H_6DO_3^+] \rightarrow H_4DO_2^+ + H_2O$ | 4.05 | 6.25 | |
| | $H_5O_2^+ + H_2O \leftarrow [H_5D_2O_3^+] \rightarrow H_4DO_2^+ + HOD$ | 40.9 | 100.0 | |
| | $H_5O_2^+ + {}^1/_2D_2O = H_4DO_2^+ + {}^1/_2H_2O$ | 12.9 | 25.0 | 0.48 |
| 1 | $H_4DO_2^+ + HOD \leftarrow [H_5D_2O_3^+] \rightarrow H_3D_2O_2^+ + H_2O$ | 0.72 | 1.0 | |
| | $H_4DO_2^+ + D_2O \leftarrow [H_4D_3O_3^+] \rightarrow H_3D_2O_2^+ + HOD$ | 8.81 | 16.0 | |
| | $H_4DO_2^+ + {}^1/_2D_2O = H_3D_2O_2^+ + {}^1/_2H_2O$ | 2.52 | 4.0 | 0.59 |
| 2 | $H_3D_2O_2^+ + HOD \leftarrow [H_4D_3O_3^+] \rightarrow H_2D_3O_2^+ + H_2O$ | 0.19 | 0.25 | |
| | $H_3D_2O_2^+ + D_2O \leftarrow [H_3D_4O_3^+] \rightarrow H_2D_3O_2^+ + HOD$ | 2.24 | 4.0 | |
| | $H_3D_2O_2^+ + {}^1/_2D_2O = H_2D_3O_2^+ + {}^1/_2H_2O$ | 0.65 | 1.0 | 0.61 |
| 3 | $H_2D_3O_2^+ + HOD \leftarrow [H_3D_4O_3^+] \rightarrow HD_4O_2^+ + H_2O$ | 0.063 | 0.0625 | |
| | $H_2D_3O_2^+ + D_2O \leftarrow [H_2D_5O_3^+] \rightarrow D_5O_2^+ + HOD$ | 0.71 | 1.0 | |
| | $H_2D_3O_2^+ + {}^1/_2D_2O = HD_4O_2^+ + {}^1/_2H_2O$ | 0.212 | 0.25 | 0.79 |
| 4 | $HD_4O_2^+ + HOD \leftarrow [H_2D_5O_3^+] \rightarrow D_5O_2^+ + H_2O$ | 0.013 | 0.010 | |
| | $HD_4O_2^+ + D_2O \leftarrow [HD_6O_3^+] \rightarrow D_5O_2^+ + HOD$ | 0.13 | 0.16 | |
| | $HD_4O_2^+ + {}^1/_2D_2O = D_5O_2^+ + {}^1/_2H_2O$ | 0.041 | 0.040 | 0.96 |

[a] Gas-phase equilibrium constants calculated from experimental product distributions (Table II). [b] Fractionation factor with respect to liquid water $(0.93)(K_{expt}/K_{stat})$.

**Table VIII.** Phenomenological Equilibrium Constants for the Stepwise Deuteration Reaction (43)

| $n$ | CID products | $K_{expt}$[a] | $K_{stat}$[b] | $\phi_n$[b] |
|---|---|---|---|---|
| 0 | $H_7O_3^+ + HOD \leftarrow [H_8DO_4^+] \rightarrow H_6DO_3^+ + H_2O$ | 9.60 | 12.25 | |
| | $H_7O_3^+ + D_2O \leftarrow [H_7D_2O_4^+] \rightarrow H_6DO_3^+ + HOD$ | 107.3 | 196.0 | |
| | $H_7O_3^+ + {}^1/_2D_2O = H_6DO_3^+ + {}^1/_2H_2O$ | 32.1 | 49 | 0.62 |
| 1 | $H_6DO_3^+ + HOD \leftarrow [H_7D_2O_4^+] \rightarrow H_5D_2O_3^+ + H_2O$ | 1.89 | 2.25 | |
| | $H_6DO_3^+ + D_2O \leftarrow [H_6D_3O_3^+] \rightarrow H_5D_2O_3^+ + HOD$ | 23.4 | 36.0 | |
| | $H_6DO_3^+ + {}^1/_2D_2O = H_5D_2O_3^+ + {}^1/_2H_2O$ | 6.65 | 9.0 | 0.68 |
| 2 | $H_5D_2O_3^+ + HOD \leftarrow [H_6D_3O_4^+] \rightarrow H_4D_3O_3^+ + H_2O$ | 0.61 | 0.69 | |
| | $H_5D_2O_3^+ + D_2O \leftarrow [H_5D_4O_4^+] \rightarrow H_4D_3O_3^+ + HOD$ | 8.14 | 11.1 | |
| | $H_5D_2O_3^+ + {}^1/_2D_2O = H_4D_3O_3^+ + {}^1/_2H_2O$ | 2.23 | 2.78 | 0.75 |
| 3 | $H_4D_3O_3^+ + HOD \leftarrow [H_5D_4O_4^+] \rightarrow H_3D_4O_3^+ + H_2O$ | 0.24 | 0.25 | |
| | $H_4D_3O_3^+ + D_2O \leftarrow [H_4D_5O_4^+] \rightarrow H_3D_4O_3^+ + HOD$ | 2.98 | 4.0 | |
| | $H_4D_3O_3^+ + {}^1/_2D_2O = H_3D_4O_3^+ + {}^1/_2H_2O$ | 0.85 | 1.0 | 0.79 |
| 4 | $H_3D_4O_3^+ + HOD \leftarrow [H_4D_5O_4^+] \rightarrow H_2D_5O_3^+ + H_2O$ | 0.088 | 0.09 | |
| | $H_3D_4O_3^+ + D_2O \leftarrow [H_3D_6O_4^+] \rightarrow H_2D_5O_3^+ + HOD$ | 1.13 | 1.44 | |
| | $H_3D_4O_3^+ + {}^1/_2D_2O = H_2D_5O_3^+ + {}^1/_2H_2O$ | 0.32 | 0.36 | 0.83 |
| 5 | $H_2D_5O_3^+ + HOD \leftarrow [H_3D_6O_4^+] \rightarrow HD_6O_3^+ + H_2O$ | 0.028 | 0.0278 | |
| | $H_2D_5O_3^+ + D_2O \leftarrow [H_2D_7O_4^+] \rightarrow HD_6O_3^+ + HOD$ | 0.37 | 0.444 | |
| | $H_2D_5O_3^+ + {}^1/_2D_2O = HD_6O_3^+ + {}^1/_2H_2O$ | 0.10 | 0.111 | 0.84 |
| 6 | $HD_6O_3^+ + HOD \leftarrow [H_2D_7O_4^+] \rightarrow D_7O_3^+ + H_2O$ | 0.0063 | 0.0051 | |
| | $HD_6O_3^+ + D_2O \leftarrow [HD_8O_4^+] \rightarrow D_7O_3^+ + HOD$ | 0.0075 | 0.0816 | |
| | $HD_6O_3^+ + {}^1/_2D_2O = D_7O_3^+ + {}^1/_2H_2O$ | 0.022 | 0.0204 | 1.0 |

[a] Gas-phase equilibrium constants calculated from experimental product distributions (Table III). [b] Fractionation factor with respect to liquid water $(0.93)(K_{expt}/K_{stat})$.

tributions are given in Table VII. The individual fractionation factors shown are derived by multiplying $K_{40}$ by 0.93 ($K_{28}$) and dividing by the appropriate statistical factors, also given in Table VII. The trend of increasing fractionation factor with increased deuterium content is reproduced for CID of the trimer. The average fractionation factor for $L_5O_2^+$ is derived from the equilibrium constant for eq 41. The resulting value of $\phi(L_5O_2^+)$

$$H_5O_2^+(g) + {}^1/_2D_2O(l) = D_5O_2^+(g) + {}^1/_2H_2O(l) \quad (41)$$

$$\phi(L_5O_2^+) = K_{41}{}^{1/5} \quad (42)$$

given by eq 42 is 0.68 ± 0.02, somewhat lower than $\phi(L_3O^+)$ derived from the product distributions of the dimer. This value is again lower than the fractionation factor of 0.73 ± 0.05 measured by Larson and McMahon for the equilibrium bimolecular exchange reaction (41); however, the difference is small and within experimental error.[27]

In Table VIII the equilibrium constants are given for the deuteration of $L_7O_3^+$ (eq 43) as derived from the experimental product distribution from CID of $L_9O_4^+$ (Table III). Also listed

$$H_{7-n}D_nO_3^+(g) + {}^1/_2D_2O(g) = H_{6-n}D_{n+1}O_3^+(g) + {}^1/_2H_2O(g) \quad (43)$$

are the associated fractionation factors. As seen for the product distribution from CID of the dimer and trimer, a trend of increasing fractionation factors with increased deuterium content is observed. An overall fractionation factor of 0.78 ± 0.02 is derived from $K_{44}$ and eq 45.

$$H_7O_3^+(g) + {}^7/_2D_2O(l) = D_7O_3^+(g) + {}^7/_2H_2O(l) \quad (44)$$

$$\phi(L_7O_3^+) = K_{44}{}^{1/7} \quad (45)$$

The increased value for $\phi(L_7O_3^+)$ compared to $\phi(L_5O_2^+)$ and $\phi(L_5O_2^+)$ is somewhat surprising because one might expect a

monotonic decrease in fractionation factors approaching the value for aqueous $L_3O^+$ (0.69). The data for the $L_9O_4^+$ cluster (Table III) are of comparable quality to those for the $L_7O_3^+$ and $L_5O_2^+$ clusters (Tables I and II, respectively) in terms of reproducibility. The sudden increase in fractionation factor observed for the tetramer may result from the accessibility of alternative low-energy structures (e.g., **6**) such that bridging and terminal positions are

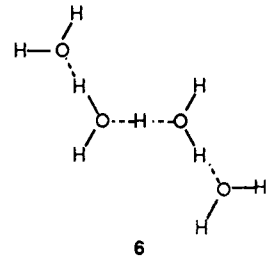

**6**

less well-defined than in **1-3**. Alternatively, the tetramer cluster may have a higher effective internal temperature, as a result either of incomplete thermal equilibration in the flow tube or of collisional activation in the lenses of the sampling system.

## Conclusions

The product distributions resulting from CID of partially deuterated water cluster ions reflect a preference for fractionation of deuterium to the neutral CID product. The fractionation appears to be independent of collision energy within experimental error and is therefore identified as resulting from an equilibrium isotope effect that acts to alter the equilibrium distribution of cluster isotopomers. This fractionation effect appears to be the same effect observed in gas-phase bimolecular isotope-exchange reactions and in condensed-phase isotope fractionation. The values for the fractionation factors of gaseous $L_3O^+$ and $L_5O_2^+$ resulting from the present data are only slightly lower than those observed for the equilibrium exchange reactions.[26,27] This difference may be a consequence of different internal energies for the cluster ions in the present study compared to the corresponding intermediates in the equilibrium reactions and/or a difference in the effective temperature at which the fractionation occurs. Fractionation factors for stepwise deuteration in each of the $(L_2O)_nL^+$ ($n$ = 2-4) species display dependence on deuterium content, increasing toward unity as the deuterium content increases. We intend to continue our study of isotope fractionation in cluster ion CID with investigations of the $NH_4^+/ND_3$ system, in which D is predicted to preferentially migrate to the *ionic* products of the bimolecular exchange reaction[32,57] and therefore should also fractionate to the ionic products of activated unimolecular decomposition. Other systems of potential interest include the anionic clusters $OL^-(L_2O)_n$ and mixed species such as $CH_3OL_2^+(L_2O)$.

**Acknowledgment.** Support of this work by the National Science Foundation (Grant CHE-8502515) is gratefully acknowledged. R.R.S. thanks the Alfred P. Sloan Foundation for a fellowship and S.T.G. acknowledges the David Ross Foundation for fellowship support.

# A Transient Infrared Spectroscopy Study of Coordinatively Unsaturated Osmium Carbonyl Compounds

**Paula L. Bogdan and Eric Weitz***

*Contribution from the Department of Chemistry, Northwestern University, Evanston, Illinois 60208.* *Received June 5, 1989*

**Abstract:** Transient infrared spectroscopy is used to study the coordinatively unsaturated osmium carbonyl fragments generated by 248-nm photolysis of gas-phase $Os(CO)_5$. The nascent photoproducts, predominantly $Os(CO)_3$ with some $Os(CO)_4$, are highly reactive toward combination with both CO and $Os(CO)_5$. The bimolecular rate constants for reaction of $Os(CO)_3$ and $Os(CO)_4$ with CO are $7.6 \pm 0.9$ and $5.5 \pm 0.6 \times 10^{-11}$ cm$^3$ molecule$^{-1}$ s$^{-1}$, respectively. Infrared absorptions for a new unsaturated osmium species, $Os_2(CO)_8$, formed by reaction of $Os(CO)_3$ with $Os(CO)_5$, are assigned. The rate constant for this reaction is $2.7 \pm 0.9 \times 10^{-10}$ cm$^3$ molecule$^{-1}$ s$^{-1}$, on the order of gas kinetic. The reactivities of the unsaturated osmium species are similar to those of the analogous ruthenium compounds and contrast with the reactivity of $Fe(CO)_4$. The trends observed in the photochemistry of group 8 metal carbonyl complexes and the role of spin selection rules in the reactivity of these coordinatively unsaturated fragments are discussed. Continuing depletion of the $Os(CO)_5$ parent after photolysis indicates that polynuclear osmium carbonyl clusters are formed.

Studies of unsaturated metal carbonyl compounds continue to be of fundamental interest because of their central role in stoichiometric and catalytic reaction processes.[1,2] An understanding of the structure and reactivity patterns of these key intermediates can be beneficial in the design of new catalysts, solid-state materials, and thin-film coatings.

Transient infrared spectroscopy is a powerful tool in the study of unsaturated metal carbonyl complexes.[3] The technique can provide both kinetic and structural information for transient species. Both gas-phase and solution-phase measurements have been performed. Advantages of gas phase studies are that multiple open coordination sites can be generated by photolysis and the species generated are free from solvation effects.

To date, a variety of metal carbonyl compounds has been investigated with transient infrared spectroscopy.[4-6] Some of the most intriguing results have been reported for photofragments of iron pentacarbonyl.[7] The rate constants for the reaction of $Fe(CO)_4$ with CO and with $Fe(CO)_5$ are approximately $10^3$

(1) Ugo, R., Ed. *Aspects of Homogeneous Catalysis*; D. Reidel: Dordrecht, The Netherlands, 1984; Vol. 5.
(2) Twigg, M. V., Ed. *Mechanisms of Inorganic and Organometallic Reactions*; Plenum Press: New York, 1986; Vol. 4, Part 3.
(3) Weitz, E.; Poliakoff, M. *Adv. Organomet. Chem.* **1986**, *25*, 277.
(4) Weitz, E. *J. Phys. Chem.* **1987**, *91*, 3945.
(5) Schaffner, K.; Grevels, F.-W. *J. Mol. Struct.* **1988**, *173*, 51.
(6) Ishikawa, Y.; Hackett, P. A.; Rayner, D. M. *J. Mol. Struct.* **1988**, *174*, 113.
(7) Poliakoff, M.; Weitz, E. *Acc. Chem. Res.* **1987**, *20*, 408.

0002-7863/90/1512-639$02.50/0 